

Influence of wind stress and discharge on the mean and seasonal currents on the Alabama shelf of the northeastern Gulf of Mexico

Brian Dzwonkowski¹ and Kyeong Park^{1,2}

Received 4 June 2010; revised 27 August 2010; accepted 1 October 2010; published 21 December 2010.

[1] Analysis of a relatively long (3.33 years) time series of velocity in 20 m of water on the Alabama shelf of the northeastern Gulf of Mexico in conjunction with long-term records of wind stress and discharge reveal a better understanding of the seasonal currents. Analysis of the mean and seasonal signals of the depth averaged velocity shows virtually no mean flow, but a relatively small yet significant seasonal signal. The 3 cm s^{-1} seasonal signal is primarily rectilinear in the along-shelf direction with peak eastward (westward) flow during the late spring (late fall), consistent with the patterns reported in previous basin scale studies of the region. The two prominent regional forcing functions, wind stress and freshwater discharge, show clear seasonal signals. The seasonal vertical profiles also show two distinctively different patterns, most clearly observed in the fall with a westward maximum flow at the surface that decreases with depth and spring with a subsurface eastward flow and a reduced westward or even eastward surface flow. Separation of the current velocity into a wind-driven component and a non-wind-driven component demonstrates their counteracting influence on the mean current and maximizes seasonal effects where the minimum (maximum) seasonal wind-driven signal roughly corresponds to the maximum (minimum) non-wind-driven signal in late spring/early summer (late fall/early winter). On the basis of several sources of indirect evidence, it is hypothesized that a freshwater discharge generated barotropic pressure gradient is the primary forcing of the seasonal signal in the non-wind-driven current.

Citation: Dzwonkowski, B., and K. Park (2010), Influence of wind stress and discharge on the mean and seasonal currents on the Alabama shelf of the northeastern Gulf of Mexico, *J. Geophys. Res.*, 115, C12052, doi:10.1029/2010JC006449.

1. Introduction

[2] Understanding the shelf circulation and the processes controlling shelf circulation is essential in determining the transport and fate of material arising in or entering the coastal zone. The seasonal current on continental shelves can often be challenging to assess because current response to seasonal forcing mechanisms can vary temporally due to interannual variability and spatially due to coastal geography as well as forcing distributions [Ullman and Codiga, 2004; Lentz, 2008a]. In order to determine the fidelity of seasonal currents, long time series are typically needed as a result of the large variability in coastal current [Lentz, 2008a]. Despite these difficulties, there are a number of studies examining seasonal circulation on continental shelves. However, the northeast region of the Gulf of Mexico and the Mississippi/Alabama (MS/AL) shelf, in particular, has received limited attention with respect to shelf circulation.

[3] The currents in the northeast Gulf of Mexico are expected to have a strong seasonal signal as the forcing functions have strong seasonal patterns. Wind stress, the primary forcing function in the region, experiences a seasonal shift from northerly directions in the winter to southerly in the summer [de Velasco and Winant, 1996; Morey *et al.*, 2005]. Regional freshwater discharge also has a clear seasonal shift with maxima occurring in late winter/early spring and minima occurring in late summer/early fall [Stumpf *et al.*, 1993; Morey *et al.*, 2005]. There is an annual cycle in the heat flux in the Gulf of Mexico [Virmani and Weisberg, 2003], from which an annual reversal of the temperature gradient occurs on account of the shallower coastal water column heating and cooling faster than the deep water offshore [Morey *et al.*, 2005]. Such a strong seasonality in the main forcing functions suggests that the regional currents may also have a strong seasonal signal.

[4] While several studies in 1980s suggest a mean westward wind-driven current in the northeastern Gulf of Mexico, these studies are based on limited current measurements, satellite images, and drifters of opportunity [Chuang *et al.*, 1982; Schroeder *et al.*, 1985, 1987]. More recent studies include He and Weisberg [2002, 2003], which examine the seasonal transition during spring and fall using a numerical model. Morey *et al.* [2003a, 2003b, 2005]

¹Dauphin Island Sea Lab, Dauphin Island, Alabama, USA.

²Dauphin Island Sea Lab, Department of Marine Sciences, University of South Alabama, Dauphin Island, Alabama, USA.

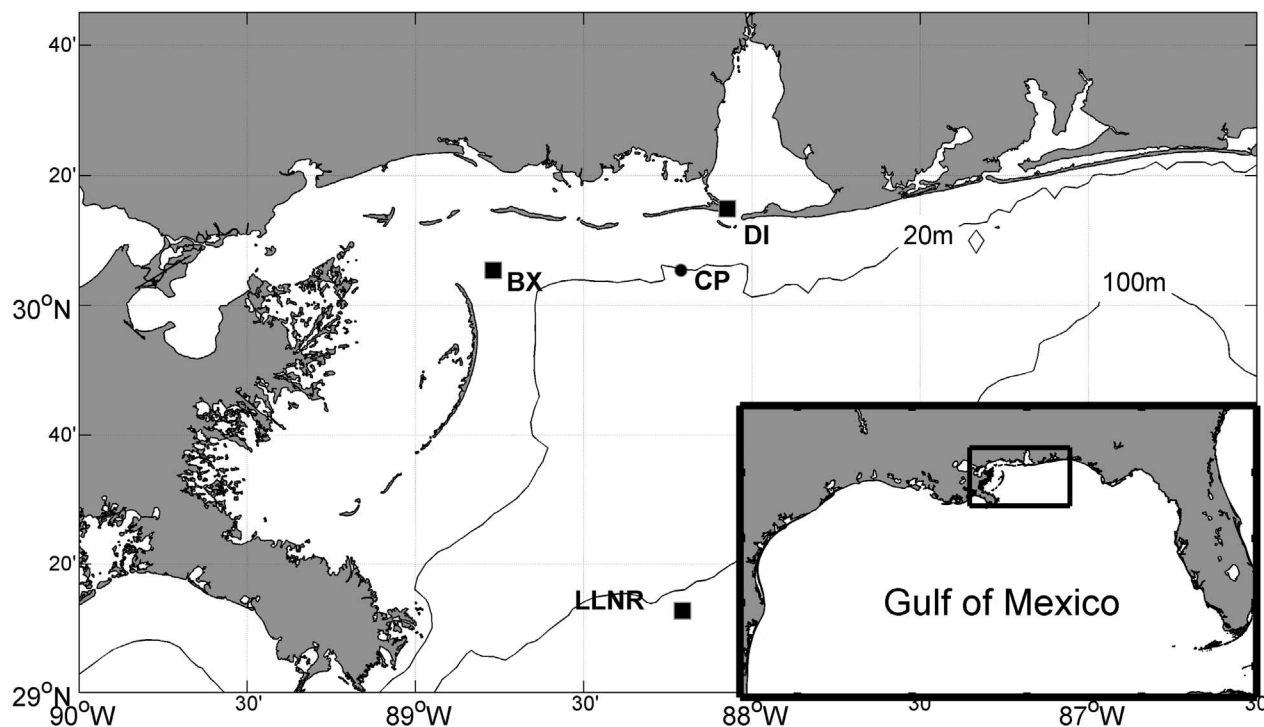


Figure 1. The study area showing the mooring station (CP) and wind stations (DI, BX, and LLNR) with a larger view of the Gulf of Mexico in the lower right corner.

examine the seasonal circulation and export of freshwater throughout the Gulf of Mexico using primarily a numerical model supported with drifters and satellite imagery. These studies show that currents along the MS/AL shelf flow eastward during the spring and summer, while westward during the fall and winter. Other studies, such as *Smith and Jacobs* [2005], only show eastward current during the spring using a time-independent model with variational data assimilation. *Ohlmann and Niiler* [2005] using 6 years of surface drifter data in the northern Gulf of Mexico makes no mention of seasonal patterns on the MS/AL shelf. While the consensus results of these more recent studies suggest a seasonal current shifting from west in fall and winter to east in spring and summer along the MS/AL shelf, all of them are basin-size in scale with only limited focus on the MS/AL shelf region. In addition, these studies only focus on the surface, bottom, or depth-averaged currents with no attention to vertical current structure, the exception being *He and Weisberg* [2002, 2003].

[5] In terms of forcing mechanisms, the previous studies have identified wind as the primary forcing mechanism responsible for the seasonal change in current direction on the MS/AL shelf [*He and Weisberg*, 2002, 2003; *Morey et al.*, 2003a, 2003b, 2005; *Smith and Jacobs*, 2005]. However, the MS/AL shelf is inundated with freshwater from the Mississippi River and Mobile Bay, respectively, the first and fourth largest sources of freshwater in the continental United States. Including other sources of freshwater such as Pascagoula River, Pearl River, and Lake Pontchartrain, freshwater discharge would certainly be expected to influence the inner to midshelf dynamics in this region. There are only a few studies that have examined the

effect of freshwater on shelf circulation in this region [e.g., *Morey et al.*, 2003a], but these studies have not focused on the inner to middle part of the MS/AL shelf.

[6] As the Deepwater Horizon oil spill illustrates, we need to have a better understanding of shelf circulation and the processes forcing seasonal current patterns in the northeastern Gulf of Mexico including the MS/AL shelf region. As such, this paper provides observational evidence of seasonal currents on the Alabama shelf and explores potential driving mechanisms for the seasonal patterns; to our knowledge, this is the first study to examine the vertical current structure on the MS/AL shelf with in situ data. This study builds on the recent basin-scale circulation studies mentioned above by quantifying the seasonal signal in a multiyear time series of current and elaborates on the previous work by examining the seasonal structure of the depth dependent currents and identifying a distinct, significant non-wind-driven contribution to the seasonal currents.

2. Data and Method

2.1. Data Sources

[7] To analyze the seasonal currents and the associated forcing mechanisms, a time series of current velocity at one station, in conjunction with regional wind velocity and river discharge from several locations were obtained (Figure 1). The current data were collected using an upward-looking ADCP at a 20 m deep mooring station located approximately 20 km offshore of Dauphin Island (station CP in Figure 1). The ADCP was deployed in November 2004 and maintained with periodic services till March 2008. Presence of data gaps resulted in approximately 2.75 years (83%) of

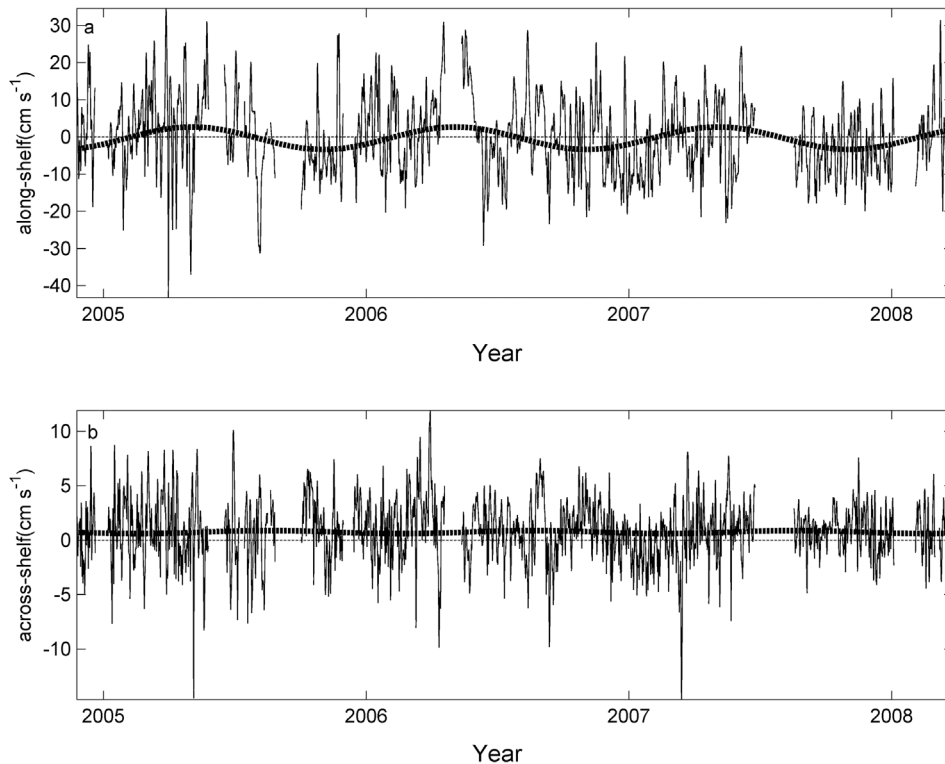


Figure 2. Depth averaged (a) along-shelf and (b) across-shelf velocity; the thick dashed lines indicate the seasonal signals derived from harmonic analysis.

data over 3.33 years of deployment. Some of the data gaps are rather large (Figure 2), O(weeks), but they are interspersed throughout the time series, resulting in a typically small percentage of gaps during any individual season; see section 2.2 for the definition of season. Data from the ADCP were collected at 0.5 m bins between 2 and 19 m above the bottom (mab), of which 2–17 mab were consistently reliable. At the start of the study during the months of November to December 2004, 2 m bins were used, followed by 1 m bins during January to March 2005.

[8] Data for forcing conditions, regional wind velocity and freshwater discharge, were obtained. Wind data during the study period and long-term records over 10 years were available at three National Data Buoy Center stations, http://www.ndbc.noaa.gov/to_station.shtml (Figure 1); however, there were gaps in these data as well. Inshore of the CP site, data from station DPIA1 (DI) were available from 1987 to 2009 with approximately 85% data coverage during this period. To the west of the CP site, data from NOAA buoy station 42007 (BX) were available from 1981 to 2009 with approximately 82% data coverage during this period. Off-shore of the site, data from NOAA buoy station 42040 (LLNR) were available from 1995 to 2008 with approximately 75% data coverage during this period. Daily discharge data were obtained for the Mississippi River at the U.S. Army Corp of Engineers' station at Tarbert Landing, MS (31°00'30"N, 91°37'25"W; <http://www.mvn.usace.army.mil/cgi-bin/wcmanual.pl?01100>), and for the Mobile River system at two U.S. Geological Survey's gauging stations for Alabama River (31°32'48"N, 87°30'45"W; http://waterdata.usgs.gov/usa/nwis/uv?site_no=02428400)

and Tombigbee River (31°45'25"N, 88°07'30"W; http://waterdata.usgs.gov/usa/nwis/uv?site_no=02469761). Data at Tarbert Landing, MS were available from 1970 to 2008 with approximately 100% data coverage during this period, and data for the Mobile River system were available from 1976 to 2008 with approximately 99% data coverage during this period. It is worth noting that of the Mississippi River discharge feeding into the “birdsfoot” delta approximately 50% affects the east side of the delta [Wiseman *et al.*, 1997].

2.2. Data Processing and Analysis

[9] Several processing techniques and analysis methods are employed in order to examine the seasonal characteristics in the data. In handling data gaps in both wind and current data, the short gaps of 12 h or less are filled using linear interpolation. Following this, all time series are low pass filtered using a 40 h Lanczos filter, similar to the filtering methods of Ullman and Codiga [2004]. The wind velocity time series are transformed into wind stress, prior to filtering, using the height of the sensor and a bulk formula of Large and Pond [1981]. From the low-pass signal, a depth averaged current is calculated as

$$\mathbf{U} = \frac{1}{h} \int_h^0 \mathbf{u}(z) dz, \quad (1)$$

where \mathbf{U} = depth averaged current, h = water depth, and $\mathbf{u}(z)$ = vertically varying current velocity. The depth integration in equation (1) is done using the trapezoidal method. The velocity data not available near the surface and bottom are

obtained by extrapolating to the surface (bottom) with a constant value from the upper (lower) most value. A linear trend from the upper (lower) values to the surface (bottom) was also performed; however, little difference resulted. The orientation of the coastline, isobath contours and the principal components of the depth averaged current warrant considering the (u, v) velocity components as the along-shelf and across-shelf components, respectively.

[10] From the depth averaged current, seasonal means are calculated for each season during the study period. The seasonal divisions follow typical midlatitude separation with winter (December to February), spring (March to May), summer (June to August), and fall (September to November). Because of data gaps, 5 out of 13 seasons have less than 80% data coverage with one (summer of 2005) having less than 60% data coverage. Similar to the criteria used in a mean seasonal analysis by *Codiga* [2005], only the seasons with at least 60% data coverage are considered in the subsequent analysis. Standard error analysis, following *Lentz* [2008b], is used to quantify the uncertainty in the seasonal means.

[11] On account of several regional studies in the northern Gulf of Mexico showing seasonal shifts in forcing functions [*Stumpf et al.*, 1993; *de Velasco and Winant*, 1996; *Virmani and Weisberg*, 2003; *Morey et al.*, 2005] and having found evidence of seasonal currents [*He and Weisberg*, 2002, 2003; *Morey et al.*, 2003a, 2003b, 2005], we attempt to quantify the seasonal signal using harmonic analysis with a single annual harmonic (see the next paragraph), following the methodology of *Lentz* [2008b]. The mean and seasonal signal in the time series is extracted by fitting the data to the form of

$$y(t) = \bar{y} + A \cdot \sin(\omega t) + B \cdot \cos(\omega t), \quad (2)$$

where y = time series, t = time in days, \bar{y} = time average, $\omega = 2\pi/(365.25 \text{ d})$ = annual frequency, and A and B = coefficients of the harmonic fit. The results can be summarized using amplitude and phase for scalar data (e.g., freshwater discharge), while vector data (e.g., current velocity and wind) can be concisely summarized using the parameters of an ellipse (major axis, minor axis, orientation of ellipse, and phase) which describe the orientation and motion of the vector. In all cases, the phases are referenced to 1 January. The confidence intervals associated with the ellipse parameters are calculated following the linear method described by *Pawlowicz et al.* [2002]. The duration and gappy nature of the data sets, however, complicate the error analysis. The error analysis uses the background level of spectral energy of the residual time series around the frequency of interest, i.e., original time series with the signals of interest removed, and the estimated error for harmonic coefficients is propagated linearly into the ellipse parameters. However, the relatively short duration of the velocity data (3.33 years) limits the discrete Fourier frequencies that can be used to ascertain the background energy around the annual frequency [*Lentz*, 2008b]. Furthermore, the level of data gaps and the relative distribution of these gaps can affect the overall spectral energy since gap filling is required so that the Fourier transform can be used to obtain spectral estimates. Thus, estimating the uncertainty in the harmonic analysis is limited and the confidence interval estimated

should be viewed as an approximate value rather than a strict significance threshold.

[12] To validate the use of a simple annual harmonic to quantify the seasonal signal, an additional analysis examining any asymmetry in the seasonal signal is conducted. This can be determined by adding higher harmonics to the least squares fit in equation (2) [*Beardsley et al.*, 1985; *Breaker*, 2005]. Additional harmonics are included incrementally to examine their individual contributions and effects on the seasonal signal. Addition of the next harmonic, the semiannual cycle with period of $365.25/2$ days, has virtually no effect on the annual harmonic and has a harmonic coefficients ($< 1 \text{ cm s}^{-1}$) only one fourth of the annual harmonic coefficients which is much smaller than its confidence interval. Additional harmonics are even smaller contributors and of less importance. This suggests that the annual harmonic is the dominant contributor to the seasonal signal despite the potential presence of other harmonics in the seasonal current. In this study, therefore, a single annual harmonic is used to quantify the dominant, and previously noted, seasonal shift in the flow pattern.

[13] Additional analysis techniques using linear correlation and regression, following *Lentz* [2008a], are used to find the wind-driven component of the depth averaged current. First, the optimum wind direction with the highest correlation with the depth averaged along-shelf current is obtained. Then, a linear regression is conducted to estimate a regression coefficient between the depth averaged along-shelf current (U_{AL}) and the optimum wind stress (τ_O^S),

$$U_{AL} = a\tau_O^S + b, \quad (3)$$

where a = regression coefficient and b = y intercept. The resulting regression coefficient and τ_O^S are then used to generate the wind-driven component of the depth averaged along-shelf current. The residual in the along-shelf current after subtracting the wind-driven component is considered as the non-wind-driven component. The same analysis is conducted for the across-shelf current with a wind component 90° from the optimum wind direction.

3. Results

3.1. Mean and Seasonal Signals

[14] The depth averaged current in Figure 2 show variability at a wide range of time scales with fluctuations in the along (across)-shelf component of ± 30 (± 10) cm s^{-1} . While these fluctuations are common in shelf currents, such large variability masks typically weaker mean and seasonal signals. Averaging over the total and seasonal periods provides a clearer picture of any very low frequency patterns in the data. First, the overall mean is nearly zero with an along (across)-shelf component of -0.4 (0.7) cm s^{-1} (Table 1 and Figure 2). The seasonal means and their uncertainty quantified following *Lentz* [2008b] are shown in Figure 3. With the standard deviations of individual seasons ranging from 7–14 and 2–4 cm s^{-1} for the along- and across-shelf components, respectively, and subtidal decorrelation time scale of approximately 3 days, the standard error in the seasonal means are typically 1.5–2 and 0.5–1 cm s^{-1} for the along- and across-shelf components, respectively. The seasonal means in Figure 3 indicate that there is notable interannual

Table 1. Harmonic Analysis Results of the Depth-Averaged Current and Its Wind-Driven and Non-Wind-Driven Components With Their Error Estimates

	Along-Shelf Mean (cm s^{-1})	Across-Shelf Mean (cm s^{-1})	Major Axis (cm s^{-1})	Minor Axis (cm s^{-1})	Orientation (deg) ^a	Phase (deg) ^b
Depth averaged	-0.4 ± 0.6	0.7 ± 0.2	3.0 ± 2.2	0.1 ± 0.5	91 ± 10	122 ± 42
Wind driven	-2.7 ± 0.4	0.1 ± 0.0	1.2 ± 0.9	-0.1 ± 0.2	100 ± 7	143 ± 40
Non-wind driven	2.2 ± 0.5	0.6 ± 0.2	2.0 ± 1.8	0.3 ± 0.5	88 ± 17	109 ± 52

^aDegree is 0 for northward current and increases clockwise for orientation.

^bDegree is 0 on January 1 for phase.

variability between individual seasons. In addition, 6 out of 12 seasonal means are near or below the uncertainty of the seasonal average, indicating the seasonal mean current can be quite small at times. However, there is evidence of a seasonal shift with eastward flow in the spring and westward flow in the fall (Figure 3). The winter and summer appear to be transitional periods with the winter showing strong westward flow for two seasons and weak northeastward flow for two seasons, and all summer seasons showing weak westward/west-northwestward flow. This seasonal pattern is further examined using harmonic analysis with an annual signal. The results suggest the presence of a rectilinear seasonal fluctuation of magnitude of 3 cm s^{-1} in the along-shelf direction, which peaks at the beginning of May (Table 1 and Figure 2) and is consistent with the pattern in the seasonal means (Figure 3).

[15] As in the depth averaged currents, the vertical profiles of along-shelf seasonal mean currents show distinct seasonal variations (Figure 4). All three fall seasons have a westward maximum flow at the surface that decreases with depth. While the winter seasons generally have profiles similar to those in the fall, two of them, winter in 2005 and 2006, have profiles with a more pronounced eastward flow at depth. The spring and summer have very different profiles, having a subsurface eastward flow with a peak at 10–14 mab and a reduced westward or even eastward flow at the surface. A reduced flow approaching zero near the bottom is common for all seasons. Similar to the relationship between fall and winter, the spring period has a quasiregular pattern while the summer appears more transitional exhibiting a weaker eastward current at depth and a stronger westward current at the surface which suggests the shift into

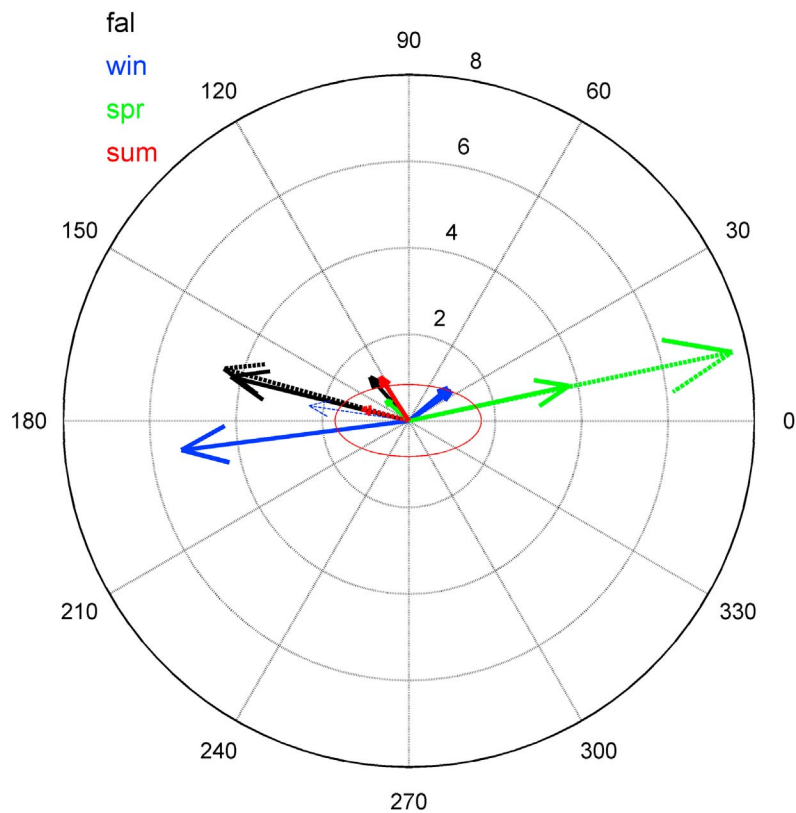


Figure 3. Seasonal mean current velocity vectors for spring (green), summer (red), fall (black), and winter (blue); the solid and dashed arrows indicate greater than 80% and 60%–80% seasonal data coverage, respectively. The concentric rings are at 2 cm s^{-1} intervals, and the red ellipse represents the approximate standard error.

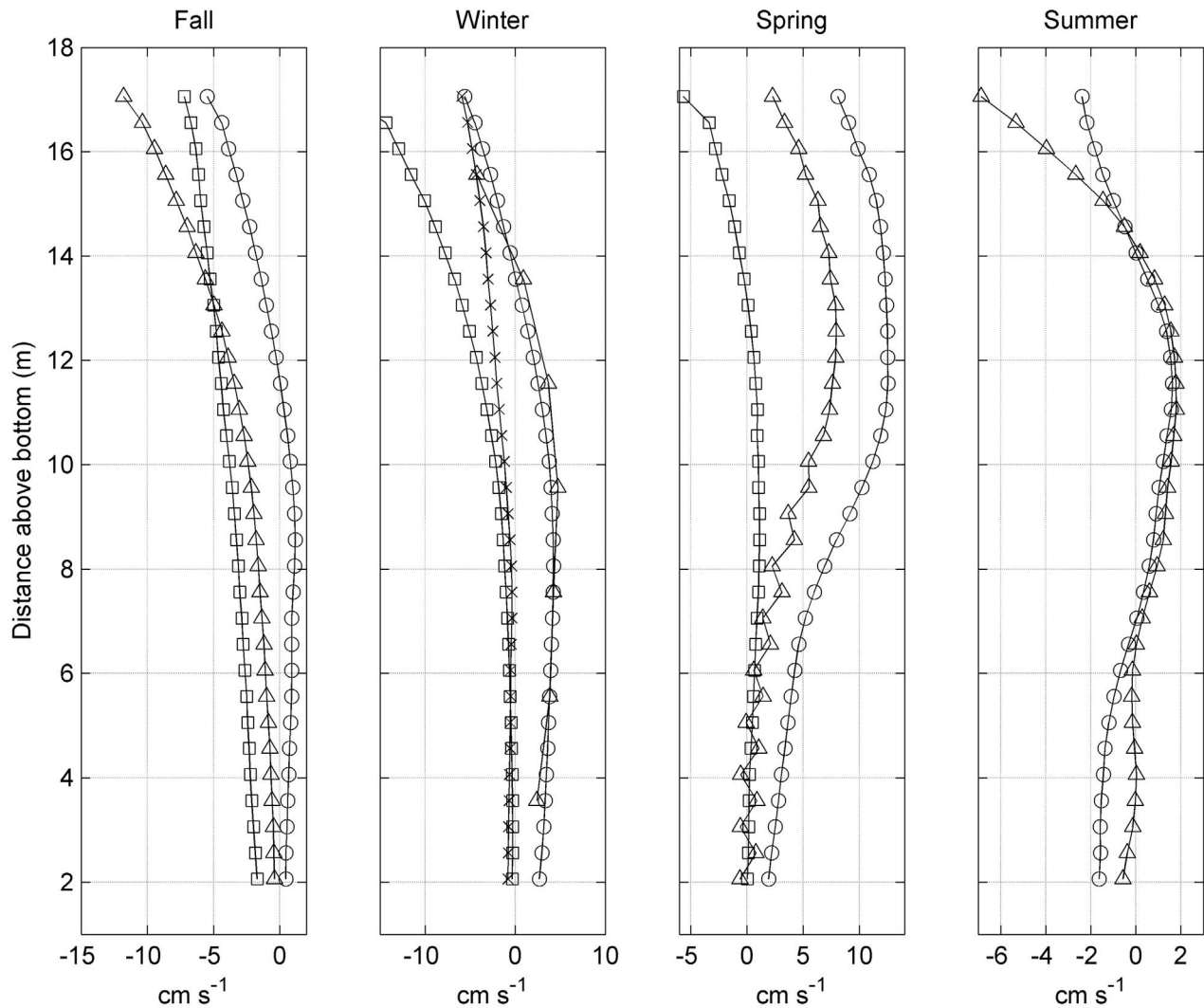


Figure 4. Seasonal depth-dependent along-shelf velocity profiles for 2005 (triangle), 2006 (circle), 2007 (square), and 2008 (cross). Note varying x axis ranges for different seasons.

the fall structure is beginning. Again, in all seasons there is considerable interannual variability in the vertical structure. It should be noted that the along-shelf current is emphasized because of the minimal role that the across-shelf current plays in the seasonal signal.

3.2. Mean Seasonal Forcing and Response

[16] Similar to the velocity data, the regional wind stress data exhibit large variability over a wide range of time scales (not shown); however, a seasonal signal exists over the 3.33 years of the study (Table 2). All three sites have a

Table 2. Harmonic Analysis Results of the Wind Stress During the Study Period and Long-Term Record^a

Stations ^b	Along-Shelf Mean (Pa)	Across-Shelf Mean (Pa)	Major Axis (Pa)	Minor Axis (Pa)	Orientation (deg) ^c	Phase (deg) ^d
<i>Study Period</i>						
DI	-0.012	-0.012	0.020	0.003	15	163
BX	-0.011	-0.009	0.022	0.002	24	165
LLNR	-0.016	-0.009	0.016	0.004	31	164
<i>Long-Term Data</i>						
DI (23 years)	-0.011 ± 0.001	-0.010 ± 0.001	0.022 ± 0.001	0.001 ± 0.002	9 ± 5	158 ± 3
BX (29 years)	-0.012 ± 0.001	-0.007 ± 0.001	0.028 ± 0.003	0.002 ± 0.004	17 ± 7	157 ± 7
LLNR (14 years)	-0.012 ± 0.002	-0.004 ± 0.002	0.018 ± 0.003	0.005 ± 0.004	19 ± 13	161 ± 12

^aThe error estimates are presented for the long-term data only.

^bSee Figure 1 for station location.

^cDegree is 0 for northward wind and increases clockwise for orientation.

^dDegree is 0 on 1 January for phase.

Table 3. Harmonic Analysis Results of the Freshwater Discharge During the Study Period and Long-Term Record^a

Rivers	Mean (m ³ s ⁻¹)	Amplitude (m ³ s ⁻¹)	Phase (deg) ^b
<i>Study Period</i>			
Mobile Bay	1236	809	57
Mississippi River ^c	12,112	6290	65
<i>Long-Term Data</i>			
Mobile Bay (33 years)	1725 ± 200	1404 ± 100	59 ± 6
Mississippi River ^c (39 years)	14,870 ± 700	7144 ± 1000	91 ± 8

^aThe error estimates are presented for the long-term data only.

^bDegree is 0 on 1 January for phase.

^cApproximately 50% of the discharge will impact the eastern region of the Mississippi birdsfoot delta [Wiseman *et al.*, 1997].

relatively rectilinear structure with the major axis being approximately 0.02 Pa and the minor axis being less than 25% of the major axis. The seasonal ellipse orientation is along 15°–31°/195°–211° with the peak northeastward/southwestward wind occurring in early May/December. The south (LLNR) and west (BX) sites, compared to DI, have a more east–west orientation. Combining this seasonal signal with the mean southwestward wind stress emphasizes the predominance of the southwestward wind conditions, particular during the late fall and early winter.

[17] The freshwater discharge from both the Mississippi River and Mobile River system has a strong seasonal signal. Harmonic analysis results show, not surprisingly, both a larger mean and seasonal signal in the Mississippi River discharge (Table 3). However, it is expected that no more than 50% of the discharge in Table 3 will impact the eastern region of the Mississippi birdsfoot delta [Wiseman *et al.*, 1997]. Both systems do have a similar phase of about 60° during the study period, i.e., the annual peak in the beginning of March.

[18] To examine the current response, if any, to these seasonal forcing functions, the depth averaged current is separated into a wind-driven component and a non-wind-driven component from which the seasonal signal is extracted using harmonic analysis. The optimal wind direction giving the highest correlation with the along-shelf current is 75° ($r = 0.63$) from which the wind-driven current is derived. The results show an interesting relationship between the mean and seasonal current of the wind-driven and non-wind-driven components. The along-shelf mean current vectors are roughly opposite in direction with the wind-driven flow directed to the west and the non-wind-driven flow directed to the east (Table 1); note the minimal contribution from the across-shelf component. The seasonal signals are mostly rectilinear, dominated by the along-shelf axis (orientation ~ 90°) with magnitudes of 1.2 and 2.0 cm s⁻¹ for the wind-driven and non-wind-driven components, respectively, and have phases separated by about a month. The oppositely directed mean wind-driven and non-wind-driven currents result in a situation in which the similarly phased seasonal signals act in an opposing manner. In late spring/early summer, a minimum wind-driven current to the west occurs with a maximum non-wind-driven current to the east, whereas in late fall/early winter a maximum wind-driven current to the west occurs with a minimum non-wind-driven current to the east (Figure 5). The net result is an east flow in late spring/early summer and a west flow in late fall/early winter (Figures 2 and 3). While a direct cause of the non-wind-driven signal is not clear from the available

data, it does follow the seasonal discharge cycle with a phase lag of about 44–52 days.

4. Discussion

[19] Our results indicate that wind stress forcing is not the only factor in determining the mean and seasonal currents, which do contain a non-wind-driven component as well as a wind-driven component.

4.1. Wind-Driven Component

[20] In regards to the wind-driven component, the mean wind stress is to the southwest (Table 2), consistent with the mean wind-driven current to the west (Table 1). The seasonality in the wind-driven current, with a maximum west current occurring in late fall/early winter (Table 1), is consistent with the corresponding seasonal vertical profiles, as they appear to be surface forced with westward friction that reduces with depth (Figure 4). While the seasonal wind stress signal orientation (15°–31° in Table 2) is not parallel to the along-shelf direction, there is a component that can drive an along-shelf current since the optimal wind stress associated with the along-shelf current is 75°, which results in a 44°–60° difference with that of seasonal wind stress orientation.

4.2. Non-Wind-Driven Component

[21] The forcing(s) associated with the non-wind-driven component is less clear and the absence of data for pressure gradients only allows for speculation based on deductive reasoning. In addition to wind stress, heat flux and discharge are expected to be important forcing functions in the Gulf of Mexico. Their seasonal cycles act to change the buoyancy forcing by alternating the baroclinic pressure gradient on the shelf. While discharge reduces the salinity on the inner shelf, seasonal heat flux typically results in colder (warmer) conditions in the shallower, inner shelf than in the deeper, outer shelf during winter (summer). During the summer the salinity and temperature gradients work in concert creating a baroclinic pressure gradient that generates a westward, downshelf current, whereas the winter gradients oppose each other and their outcome is difficult to determine without data [Morey *et al.*, 2005]. This process has been identified in various coastal shelves in He and Weisberg [2002], Ullman and Codiga [2004], Shearman and Lentz [2003, 2007], Lentz [2008a], etc. However, the westward current that would be driven by baroclinic forcing during the spring (peak discharge) and summer (peak heat flux) is not present in the non-wind-driven component of the depth average current (Figure 5), nor in the seasonal mean vertical

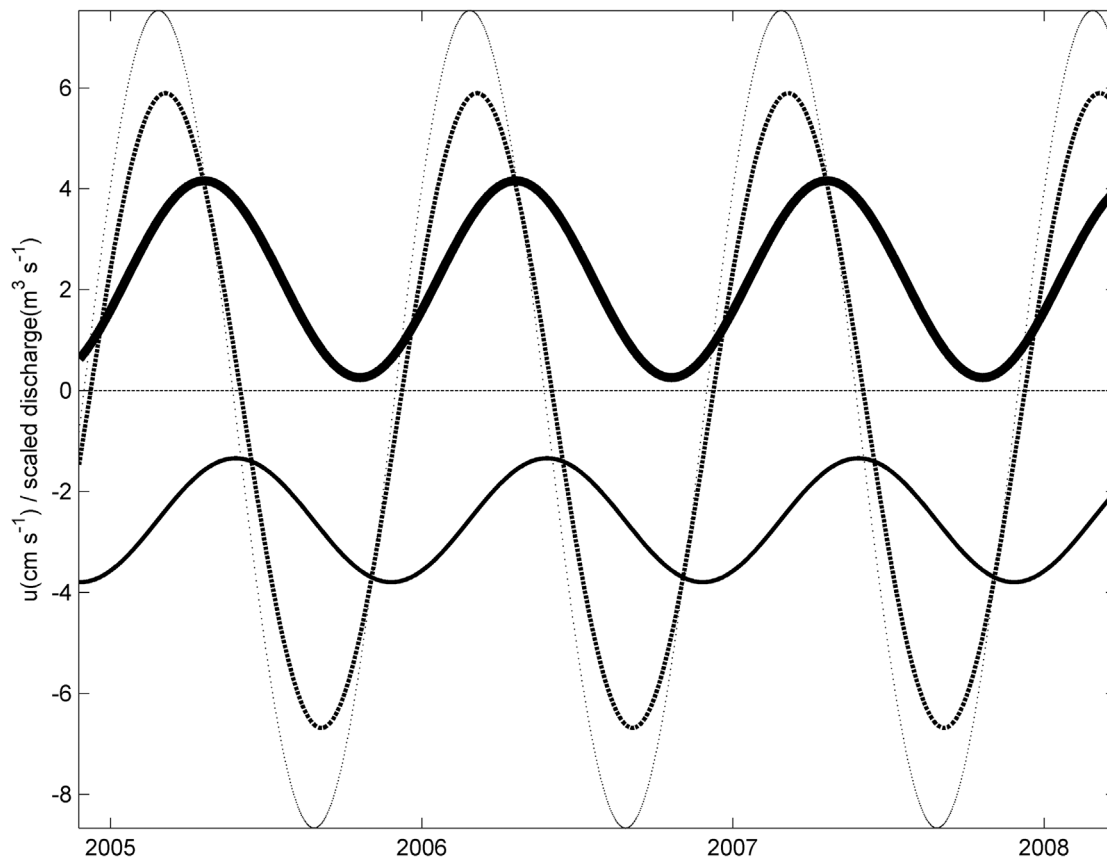


Figure 5. Seasonal signal of the wind-driven current (thin solid line), the non-wind-driven current (thick solid line), and the discharges from Mississippi River (dashed line) and Mobile River system (dotted line). The Mississippi River (Mobile River system) discharge has had the mean removed and been scaled by 1/1000 (1/100) to show the coincident fluctuations.

profiles (Figure 4). The known regional forcing mechanisms fail to provide adequate explanation for the observed non-wind-driven component.

[22] We hypothesize that the non-wind-driven component is driven by a barotropic pressure gradient related to freshwater discharge. While no data are presently available for the barotropic pressure gradient, this hypothesis is supported by several sources of indirect information including the seasonal freshwater discharge, the seasonal variation in salinity gradient, the velocity profiles, and consistency with previous studies on regional circulation.

[23] The seasonal peak in discharge from Mississippi River and Mobile Bay leads the non-wind-driven depth averaged current by about 44–52 days (Figure 5), which seems a reasonable lead time for freshwater to propagate from the gauging stations through their respective estuaries onto the shelf. In line with this seasonal cycle in discharge, previous studies in the region show strong seasonal changes in the along-shelf salinity gradient with relatively fresh and warm water accumulating on the MS/AL shelf region in late spring/early summer but the signal is much weaker in late fall/early winter (see *Jochens et al.* [2002, Figures 7.2-2, 7.2-4, and 7.2-6], *He and Weisberg* [2002, Figure 9, 2003, Figure 14], and *Morey et al.* [2003a, Figure 7, 2003b, Figure 2]). In these studies, the observed and modeled along-shelf surface salinity differences between the MS/AL

shelf and just west of Apalachicola Bay can be quite strong ranging from 4 to 8 psu. The accumulation of fresher water may cause a seasonally varying barotropic along-shelf pressure gradient that drives the observed eastward currents in late spring/early summer.

[24] The vertical structure of the seasonal velocity in spring and summer is characterized by a shape that is not consistent with a sole surface wind forcing. During the spring and to a weaker extent summer, when wind stress is at its minimum, the depth dependent current profiles have a shape consistent with a flow dominated by a barotropic pressure gradient, with some evidence of surface wind forcing acting in the opposite direction (Figure 4). Assuming wind stress and a discharge-induced pressure gradient are the two primary forcing functions on the mean and seasonal currents, idealized first-order profiles of wind-driven and barotropic pressure gradient-driven flows are generated using simple parabolic functions required to match the approximate mean depth averages of the wind-driven (Figure 6a) and non-wind-driven (Figure 6b) components. The summation of these profiles (Figure 6c) compares well to the observed mean vertical profile (Figure 6d). There are some differences, such as the depth of the eastward subsurface velocity peak, but as a very simple first-order approximation, the profiles are surprisingly similar, suggesting a pressure

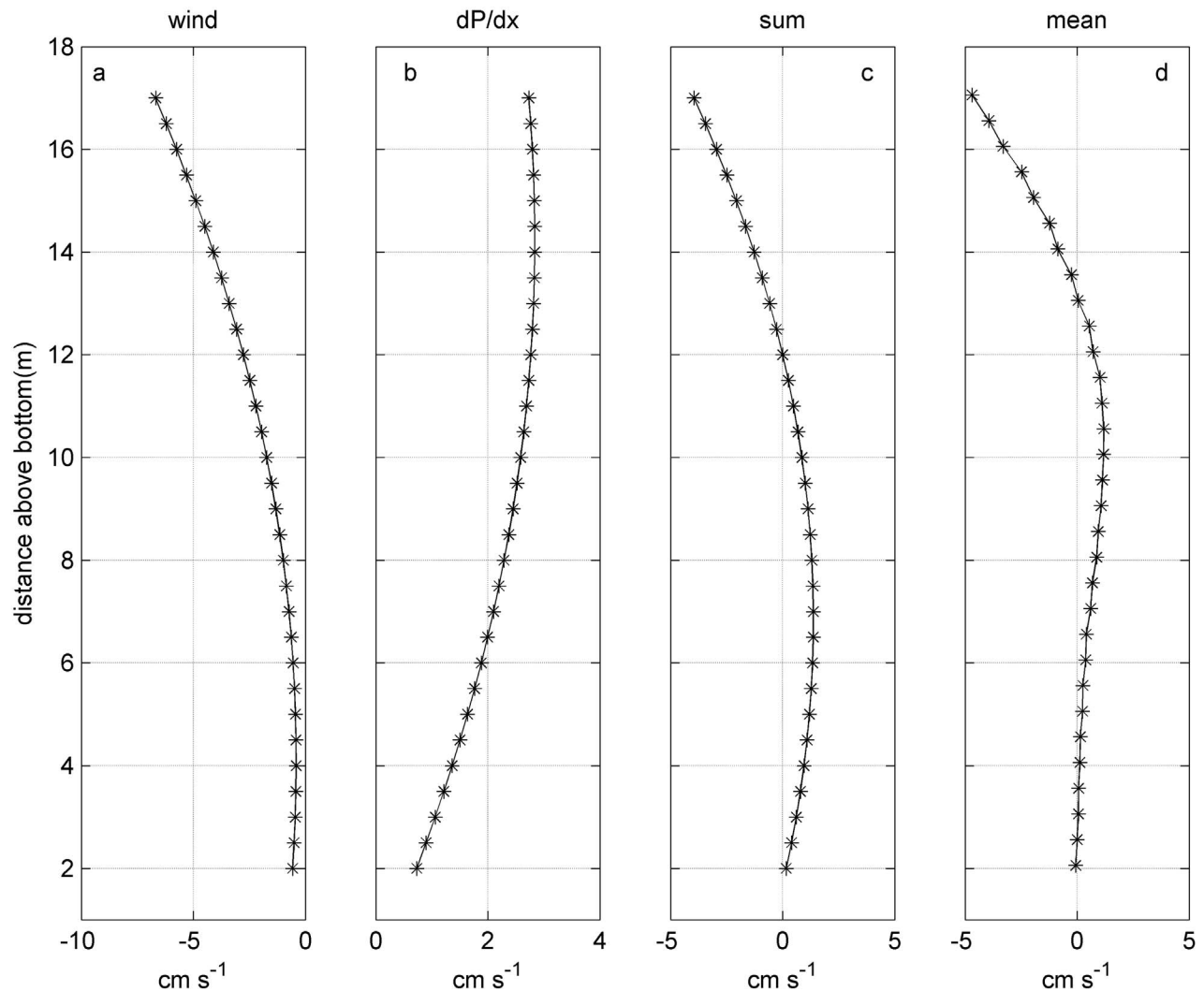


Figure 6. Idealized profiles of (a) a wind-driven current, (b) a barotropic pressure gradient–driven current and (c) their sum, and (d) the mean vertical profile from the entire time series with 0.5 m bins. The idealized vertical profiles in Figures 6a and 6b are generated using simple parabolic functions required to match the approximate mean depth averages of the wind-driven and non-wind-driven components. Note varying x axis ranges for different plots.

gradient, regardless of its source(s), is a reasonable contributor to the observed currents.

[25] Finally, the interaction between the wind-driven and non-wind-driven components appears consistent with the finding by *Morey et al.* [2003a] in which the model runs using average and seasonal discharge had similar seasonal surface salinity patterns. At first glance the similar effect of seasonal and constant discharge appears counter to our hypothesis. However, when assuming that the non-wind-driven current is completely forced by a discharge-driven barotropic pressure gradient, a constant freshwater discharge would result in a constant non-wind-driven current of about 2.2 cm s^{-1} , the along-shelf mean of the non-wind-driven component (Table 1). Then, during the late fall when the westward wind-driven component is maximum ($> 2.2 \text{ cm s}^{-1}$ in Figure 5), one could expect the transport to the west consistent with *Morey et al.* [2003a, Figure 9d]. On the other hand, when the seasonal wind-driven signal is at its mini-

mum in late spring/early summer, the constant non-wind-driven component to the east would overcome the wind forcing, resulting in eastward transport consistent with *Morey et al.* [2003a, Figure 9c].

4.3. Long-Term Variability in Forcing Function

[26] The consistency of the seasonal signal maybe questioned by the limited duration of our data set (3.33 years). As a way to examine potential changes to the seasonal signal in the current, long-term time series of wind stress and discharge are examined to see how representative the forcing conditions during our study period are. The harmonic analysis results using the long-term wind stress data show little difference in the seasonal signal from that in the wind stress data during the study period (Table 2). The harmonic analysis results using the long-term freshwater discharge presented in Table 3 show two differences that may be potentially important. The peak discharge from

Mississippi River in the long-term record occurs about a month later than during the study period. Another difference is that the study period is relatively dry compared to the long-term record; 2007, in particular, was a 30 year record dry year for the Mobile River system. Such a low discharge condition implies that the influence of freshwater discharge might be stronger during normal years. These differences, however, would only shift the timing and strength of the non-wind-driven component. Considering the relatively minor differences between the seasonal signals of the long-term and study period forcing conditions, the observed mean and seasonal signals in the current data set are expected to be relatively robust.

4.4. Monthly and Interannual Variability

[27] To gain additional confidence in the observed signal, we repeat some analysis with the monthly averaged time series. A range (60%–90%) of data coverage for monthly means of depth averaged current is examined, but the results do not qualitatively change. The seasonal signal in the monthly mean current data is similar to the hourly data, $O(3 \text{ cm s}^{-1})$. In addition, significant correlations arise between the monthly current and both wind stress, $O(0.65)$, and discharge, $O(0.4)$. The monthly time series of the along-shelf current have considerable interannual variability similar to those in Figure 3. Wind stress and discharge also have considerable interannual variability. Unfortunately, the duration of the study period limits our ability to address interannual variability of the currents and forcing. Not surprisingly, there does appear to be an association between the interplay of the interannual variability of wind and discharge and the resulting current. Some of the variability in the vertical current structure appears to be influenced by interannual variability. For example, the spring of 2007 showing quite different vertical profile with a reduced eastward flow (Figure 4) corresponds to a spring period with relatively strong southeastward wind which would act against the effect of already very low freshwater discharge. Similar interaction between wind stress and discharge appears to explain other seasonal exceptions in the vertical profiles. However, more thorough analysis of the interannual variability using longer time series is left for future work.

5. Summary and Conclusions

[28] Mean and seasonal signal in the depth averaged and dependent structure are estimated at a mooring station on the 20 m isobath on the Alabama shelf. There is virtually no mean along-shelf flow at the study site. However, there is a 3 cm s^{-1} seasonal signal in the depth averaged time series, and it is primarily rectilinear in the along-shelf direction with peak eastward (westward) flow during the late spring (late fall), consistent with the patterns observed/simulated in previous basin scale studies. Furthermore, the seasonal vertical profiles appear to have two distinctively different patterns, most clearly observed in the fall and spring. In all seasons, the seasonal depth averaged mean and the depth-dependent profiles show considerable interannual variability, which emphasizes the need for long-term time series.

[29] Wind stress and freshwater discharge, the two most prominent regional forcing functions, also show seasonality. The orientation of the seasonal wind stress signal is directed

approximately along the north-northeast/south-southwest axis, which allows it to enhance/reduce the mean current. Separation of the current velocity into a wind-driven component and a non-wind-driven component demonstrates their counteracting influence on the mean current and maximizes seasonal effects where the minimum (maximum) seasonal wind-driven signal roughly corresponds to the maximum (minimum) non-wind-driven signal in late spring/early summer (late fall/early winter). While the mean and seasonal signal in the wind-driven component corresponds well to the mean and seasonal wind patterns, forcing mechanisms for the non-wind-driven mean and seasonal signal are not obvious. From the evidence in the discharge data, seasonal variation in salinity gradient, vertical current profiles, and previous studies in the region, it is hypothesized that a freshwater discharge-generated barotropic pressure gradient is the primary forcing of the seasonal signal in the non-wind-driven current. This is different from the previous studies in other shelf regions where the influence of buoyancy forcing affects seasonal currents such that it enhances downshelf current during times of high freshwater discharge. Assuming discharge is responsible for the non-wind-driven component, the seasonal signals for long-term time series of wind stress and discharge show little difference from those of the study period, suggesting that the observed mean and seasonal signals are relatively robust. This mean and seasonal interplay between the wind-driven and non-wind-driven components is what drives the resulting current. In addition, the interannual variability in wind stress and discharge is consistent with the interannual variability in the seasonal mean currents and their depth dependent profiles.

[30] While the results of this study are based on the data from a single mooring location, which may make broader generalizations about the shelf behavior questionable, the depth averaged observations are consistent with several broader basin scale studies in the region [Morey *et al.*, 2003a, 2003b; He and Weisberg, 2002, 2003], which at least suggests that this results may apply to the much wider region of the MS/AL shelf and presents a topic of future research. The hypothesis of a seasonally strengthening barotropic pressure gradient induced by freshwater discharge could be an important mechanism in other shelf regions with high river discharge.

[31] **Acknowledgments.** This work would not have been possible without the collecting and archiving of the data by the Tech Support Group at the Dauphin Island Sea Lab, including Kyle Weis, Alan Gunter, Mike Dardeau, and Laura Linn. This work was supported by the Fisheries Oceanography in Coastal Alabama funded by Alabama Department of Conservation and Natural Resources, Marine Resources Division. Finally, we thank Rich Pawlowicz at University of British Columbia for the freely available Matlab *m_map* toolbox, which was useful in our analysis of geophysical data.

References

- Beardeley, R. C., D. C. Chapman, K. H. Brink, S. R. Ramp, and R. Schlitz (1985), The Nantucket shoals flux experiment (NSFE79): Part I. A basic description of the current and temperature variability, *J. Phys. Oceanogr.*, *15*, 713–748.
- Breaker, L. C. (2005), What's happening in Monterey Bay on seasonal to interdecadal time scales, *Cont. Shelf Res.*, *25*, 1159–1193, doi:10.1016/j.csr.2005.01.003.

- Chuang, W., W. W. Schroeder, and W. J. Wiseman Jr. (1982), Summer current observations off the Alabama coast, *Contrib. Mar. Sci.*, *25*, 121–131.
- Codiga, D. L. (2005), Interplay of wind forcing and buoyant discharge off Montauk Point: Seasonal changes in velocity structure and a coastal front, *J. Phys. Oceanogr.*, *35*, 1068–1085.
- de Velasco, G. G., and C. D. Winant (1996), Seasonal patterns of wind stress and wind stress curl over the Gulf of Mexico, *J. Geophys. Res.*, *101*(C8), 18,127–18,140, doi:10.1029/96JC01442.
- He, R., and R. H. Weisberg (2002), West Florida shelf circulation and temperature budget for the 1999 spring transition, *Cont. Shelf Res.*, *22*, 719–748.
- He, R., and R. H. Weisberg (2003), West Florida shelf circulation and temperature budget for the 1998 fall transition, *Cont. Shelf Res.*, *23*, 777–800, doi:10.1016/S0278-4343(03)00028-1.
- Jochens, A. E., S. F. DiMarco, W. D. Nowlin Jr., R. O. Reid, and M. C. Kennicutt II (2002), Northeastern Gulf of Mexico chemical oceanography and hydrography study: Synthesis report, U.S. Dep. of the Interior, Minerals Management Service, Gulf of Mexico OCS Region, New Orleans, LA.
- Large, W. G., and S. Pond (1981), Open ocean momentum flux measurements in moderate to strong winds, *J. Phys. Oceanogr.*, *11*, 324–336.
- Lentz, S. J. (2008a), Observations and a model of the mean circulation over the Middle Atlantic Bight continental shelf, *J. Phys. Oceanogr.*, *38*, 1203–1221, doi:10.1175/2007JPO3768.1.
- Lentz, S. J. (2008b), Seasonal variations in the circulation over the Middle Atlantic Bight continental shelf, *J. Phys. Oceanogr.*, *38*, 1486–1500, doi:10.1175/2007JPO3767.1.
- Morey, S. L., P. J. Martin, J. J. O'Brien, A. A. Wallcraft, and J. Zavala-Hidalgo (2003a), Export pathways for river discharged fresh water in the northern Gulf of Mexico, *J. Geophys. Res.*, *108*(C10), 3303, doi:10.1029/2002JC001674.
- Morey, S. L., W. W. Schroeder, J. J. O'Brien, and J. Zavala-Hidalgo (2003b), The annual cycle of riverine influence in the eastern Gulf of Mexico basin, *Geophys. Res. Lett.*, *30*(16), 1867, doi:10.1029/2003GL017348.
- Morey, S. L., J. Zavala-Hidalgo, and J. J. O'Brien (2005), The seasonal variability of continental shelf circulation in the northern and western Gulf of Mexico from a high-resolution numerical model, in *Circulation of the Gulf of Mexico: Observations and Models*, *Geophys. Monogr. Ser.*, vol. 161, edited by W. Sturges and A. Lugo-Fernandez, pp. 203–218, AGU, Washington, D.C.
- Ohlmann, J. C., and P. P. Niiler (2005), Circulation over the continental shelf in the northern Gulf of Mexico, *Prog. Oceanogr.*, *64*, 45–81, doi:10.1016/j.pocean.2005.02.001.
- Pawlowicz, R., R. Beardsley, and S. Lentz (2002), Classical tidal harmonic analysis including error estimates in MATLAB using T_TIDE, *Comput. Geosci.*, *28*, 929–937.
- Schroeder, W. W., O. K. Huh, L. J. Rouse Jr., and W. J. Wiseman Jr. (1985), Satellite observations of the circulation east of the Mississippi Delta: Cold-air outbreak conditions, *Remote Sens. Environ.*, *18*, 49–58.
- Schroeder, W. W., S. P. Dinnel, W. J. Wiseman Jr., and W. J. Merrell Jr. (1987), Circulation patterns inferred from the movement of detached buoys in the eastern Gulf of Mexico, *Cont. Shelf Res.*, *7*, 883–894.
- Shearman, R. K., and S. J. Lentz (2003), Dynamics of mean and subtidal flow on the New England shelf, *J. Geophys. Res.*, *108*(C8), 3281, doi:10.1029/2002JC001417.
- Shearman, R. K., and S. J. Lentz (2007), Correction to “Dynamics of mean and subtidal flow on the New England shelf”, *J. Geophys. Res.*, *112*, C02015, doi:10.1029/2006JC004074.
- Smith, S. R., and G. A. Jacobs (2005), Seasonal circulation fields in the northern Gulf of Mexico calculated by assimilating current meter, shipboard ADCP, and drifter data simultaneously with the shallow water equations, *Cont. Shelf Res.*, *25*, 157–183, doi:10.1016/j.csr.2004.09.010.
- Stumpf, R. P., G. Gelfenbaum, and J. R. Pennock (1993), Wind and tidal forcing of a buoyant plume, Mobile Bay, Alabama, *Cont. Shelf Res.*, *13*, 1281–1301.
- Ullman, D. S., and D. L. Codiga (2004), Seasonal variation of a coastal jet in the Long Island Sound outflow region based on HF radar and Doppler current observations, *J. Geophys. Res.*, *109*, C07S06, doi:10.1029/2002JC001660.
- Virmani, J. I., and R. H. Weisberg (2003), Features of the observed annual ocean-atmosphere flux variability on the West Florida Shelf, *J. Clim.*, *16*, 734–745.
- Wiseman, W. J., N. N. Rabalais, R. E. Turner, S. P. Dinnel, and A. MacNaughton (1997), Seasonal and interannual variability within the Louisiana coastal current: Stratification and hypoxia, *J. Mar. Syst.*, *12*, 237–248.

B. Dzwonkowski and K. Park, Dauphin Island Sea Laboratory, 101 Bienville Blvd., Dauphin Island, AL 36528, USA. (briandz@disl.org)